Porin proteins have critical functions in mitochondrial phospholipid metabolism in yeast

Received for publication, August 16, 2018, and in revised form, September 19, 2018 Published, Papers in Press, September 20, 2018, DOI 10.1074/jbc.RA118.005410

Non Miyata[1], **Satoru Fujii, and Osamu Kuge**[2]

From the Department of Chemistry, Faculty of Science, Kyushu University, Fukuoka 819-0395, Japan

Edited by George M. Carman

Mitochondrial synthesis of cardiolipin (CL) and phosphatidylethanolamine requires the transport of their precursors, phosphatidic acid and phosphatidylserine, respectively, to the mitochondrial inner membrane. In yeast, the Ups1–Mdm35 and Ups2–Mdm35 complexes transfer phosphatidic acid and phosphatidylserine, respectively, between the mitochondrial outer and inner membranes. Moreover, a Ups1-independent CL accumulation pathway requires several mitochondrial proteins with unknown functions including Mdm31. Here, we identified a mitochondrial porin, Por1, as a protein that interacts with both Mdm31 and Mdm35 in budding yeast (*Saccharomyces cerevisiae*). Depletion of the porins Por1 and Por2 destabilized Ups1 and Ups2, decreased CL levels by ~90%, and caused loss of Ups2-dependent phosphatidylethanolamine synthesis, but did not affect Ups2-independent phosphatidylethanolamine synthesis in mitochondria. Por1 mutations that affected its interactions with Mdm31 and Mdm35, but not respiratory growth, also decreased CL levels. Using HeLa cells, we show that mammalian porins also function in mitochondrial CL metabolism. We conclude that yeast porins have specific and critical functions in mitochondrial phospholipid metabolism and that porin-mediated regulation of CL metabolism appears to be evolutionarily conserved.

Eukaryotic cells are compartmentalized into various membrane-bounded structures, so-called organelles. Each organelle exhibits a specific lipid composition which is essential for the function and morphology of the organelle. Phospholipids, the fundamental structural elements of biological membranes, are mainly synthesized in the endoplasmic reticulum (ER)[3] and mitochondria, and then are distributed throughout the cells (1, 2).

Mitochondria are bounded by two distinct membranes, the mitochondrial inner (MIM) and outer (MOM) membranes. The MIM is the site of synthesis of a phospholipid, cardiolipin (CL), and a part of cellular phosphatidylethanolamine (PE) (3–7). In animals and yeasts, CL is synthesized from phosphatidic acid (PA) through four enzymatic reactions and PE is produced through decarboxylation of phosphatidylserine (PS) by Psd1 in the MIM (5, 8). Because mitochondria have no capacity to synthesize PS and PA *de novo*, and PS and the majority of PA are synthesized in the ER, these phospholipids should be transported from the ER to the MIM via the MOM for mitochondrial PE and CL synthesis. In the budding yeast, *Saccharomyces cerevisiae*, phospholipid transport between the ER and the MOM is thought to occur at the membrane contact sites formed by membrane-tethering complexes such as the ER-mitochondria encounter structure (ERMES) complex and the ER membrane protein complex (EMC) (9, 10).

Intermembrane space (IMS) protein complexes Ups1–Mdm35 and Ups2–Mdm35 are able to mediate phospholipid transport between the MOM and the MIM (11–14). Ups1–Mdm35 transports PA for CL synthesis, whereas Ups2–Mdm35 transports PS for PE synthesis. Mdm35, a cofactor of both Ups1 and Ups2, is required for their efficient import into the IMS and stability (15, 16). Deletion of *UPS1* leads to a remarkable (~80%) decrease in the cellular CL level (17, 18), indicating that Ups1–Mdm35 is involved in the major PA transport pathway in the IMS. Ups2–Mdm35 functions specifically in respiration-active mitochondria. When yeasts are growing logarithmically in fermentable carbon sources such as glucose, depletion of Ups2–Mdm35 has little effect on intramitochondrial PS transport and PE synthesis. However, after yeasts have consumed all the glucose and undergo a diauxic shift, namely, the metabolic transition from glycolytic fermentation to respiration, Ups2–Mdm35–mediated PS transport becomes responsible for 40–50% of PE synthesis in mitochondria (14). In addition, the mitochondrial contact site (MICOS) complex forming the intramitochondrial membrane contact sites (19) has been reported to be involved in PE synthesis from PS (13).

Deletion of *UPS2* restores CL synthesis in *ups1*Δ cells (17, 18). Thus, a Ups1-independent CL synthetic pathway has been

This work was supported by the Japan Society for the Promotion of Science KAKENHI Grants 16K07354 (to O. K.) and 17K15120 (to N. M.), the Takeda Science Foundation (to N. M.), the Naito Foundation (to N. M.), the Yamada Science Foundation (to N. M.), the Ono Medical Research Foundation (to N. M.), and Grant-in-Aid from the Tokyo Biochemical Research Foundation (to O. K.). The authors declare that they have no conflicts of interest with the contents of this article.

This article contains Figs. S1–S5 and Tables S1 and S2.

[1] To whom correspondence may be addressed: Motooka 744, Nishi-ku, Fukuoka, Fukuoka 819-0395, Japan. Tel.: 81-92-802-4162; Fax: 81-92-802-4126; E-mail: miyata@chem.kyushu-univ.jp.

[2] To whom correspondence may be addressed: Motooka 744, Nishi-ku, Fukuoka, Fukuoka 819-0395, Japan. Tel.: 81-92-802-4160; Fax: 81-92-802-4126; E-mail: kuge@chem.kyushu-univ.jp.

[3] The abbreviations used are: ER, endoplasmic reticulum; CL, cardiolipin; co-IP, co-immunoprecipitation; Dox, doxycycline; DSP, 3,3′-dithiobis(succinimidyl propionate); 4m cell, *psd2*Δ *dpl1*Δ *cho2*Δ *opi3*Δ cell; IMS, intermembrane space; MIM, mitochondrial inner membrane; MOM, mitochondrial outer membrane; NAPE, *N*-acylphosphatidylethanolamine; PA, phosphatidic acid; PC, phosphatidylcholine; PE, phosphatidylethanolamine; PG, phosphatidylglycerol: PI, phosphatidylinositol; PL, phospholipid; PS, phosphatidylserine; SD, synthetic dextrose.

suggested. Recently, we found that three inner membrane proteins, Fmp30, Mdm31, and Mdm32, are required for the Ups1-independent CL accumulation pathway under low mitochondrial PE conditions such as Ups2- or Psd1-deficient conditions. Fmp30 exhibits homology to mammalian *N*-acylphosphatidylethanolamine (NAPE)-specific phospholipase D that catalyzes the conversion of NAPE to PA and *N*-acylethanolamine, exposing its putative catalytic domain to the IMS. Mdm31 and Mdm32 exhibit homology with each other. Furthermore, overexpression of Mdm31 partially restores cell growth and CL synthesis in *ups1*Δ cells (20), consistent with the finding that Mdm31 functions in the Ups1-independent CL accumulation pathway. However, the precise mechanism by which these proteins function in CL accumulation under low mitochondrial PE conditions remains unknown.

In this study, we identified the mitochondrial outer membrane porin protein Por1 (YVDAC1) as a protein interacting with Mdm31. Por1 is a well-characterized channel-forming protein and has a paralog, Por2 (21–23). We show that the yeast porin proteins Por1 and Por2 have specific functions in mitochondrial phospholipid metabolism and that mammalian porin proteins have similar functions to those of yeast ones.

Results

Mdm31 interacts with Por1

Mdm31 and Mdm32 each have an N-terminal matrix-targeting presequence, and two transmembrane domains, one at the C terminus and one near the N terminus of the mature protein (24). Both transmembrane domains of both Mdm31 and Mdm32 span the MIM, exposing the middle regions of the proteins between the two transmembrane domains to the IMS (20, 24). To identify the interacting proteins for Mdm31 and Mdm32, we constructed multi-copy plasmids, pRS424-*FLAG-MDM31* and pRS424-*FLAG-MDM32*, encoding, respectively, Mdm31 and Mdm32 with a FLAG tag immediately after their presequences (FLAG-Mdm31 and FLAG-Mdm32).

Mitochondria from WT yeast cells carrying pRS424, pRS424-*FLAG-MDM31*, or pRS424-*FLAG-MDM32* were solubilized with a mild detergent, digitonin, and then subjected to immunoprecipitation with anti-FLAG agarose beads. The immunoprecipitates were then analyzed by SDS-PAGE and silver staining. For the FLAG-Mdm31 immunoprecipitation fraction, only a few bands were specifically detected and a ~28-kDa protein was identified as the major band, whereas for the FLAG-Mdm32 immunoprecipitation fraction, numerous bands were detected (Fig. 1*A*). Through in-gel digestion and MS, the ~28-kDa protein that was co-precipitated with Mdm31 was identified as Por1. The results of MS were confirmed by immunoblotting with anti-Por1 antibodies (Fig. 1*B*). Interestingly, the immunoblotting showed that Por1 was co-immunoprecipitated with FLAG-Mdm31 but not FLAG-Mdm32 (Fig. 1*B*), suggesting specific binding of Por1 and Mdm31. The co-immunoprecipitation of Por1 with FLAG-Mdm31 was surprising, because Por1 is an MOM-resident protein, whereas Mdm31 is an MIM-resident one. Therefore, there was a possibility that these proteins residing in spatially distinct compartments associated with each other after solubilization of mitochondria with digitonin. To assess this possibility, we treated intact mitochondria with a cross-linker, 3,3′-dithiobis(succinimidyl propionate) (DSP), followed by immunoprecipitation under denaturing conditions. Por1 was not co-immunoprecipitated with FLAG-Mdm31 without DSP treatment, whereas Por1 was clearly co-immunoprecipitated with FLAG-Mdm31 with DSP treatment (Fig. 1*C*), suggesting that Por1 intrinsically associates with Mdm31 in intact mitochondria.

Depletion of porin proteins affects CL synthesis

Next, we investigated the functions of porin proteins of yeast in CL metabolism. Yeast mitochondria harbor two porin proteins, Por1 and Por2 (23). *por1*Δ *por2*Δ double deletion mutant cells are viable, but their growth rate is very low. To minimize indirect effects and to facilitate cell manipulation, we established *por1*Δ *tetO*$_7$-*POR2* cells (designated as *tet-POR* cells), which lacked *POR1* and carried a doxycycline-repressible *POR2* gene (25). As shown in Fig. S1, during 18-h cultivation in the presence of 10 μg/ml doxycycline, *tet-POR* cells were able to grow well, although they exhibited a slightly lower growth rate than that of WT cells. As a reference, the growth rate of *ups1*Δ cells was also examined. *tet-POR* cells grew even faster than *ups1*Δ cells under these culture conditions (Fig. S1).

We examined the cellular phospholipid composition in logarithmically growing WT and *tet-POR* cells. WT and *tet-POR* cells (initial A_{600}, 0.015) were labeled with [^{32}P]P$_i$ for 12 h in YPD in the absence or presence of 10 μg/ml doxycycline. In the absence of doxycycline, the CL level in *tet-POR* cells was about 60% of that in WT cells (Fig. 2, *A* and *B*, *lanes 1* and *2*). In the presence of doxycycline, the CL level in *tet-POR* cells was further reduced to ~10% as compared with that in WT cells (Fig. 2, *A* and *B*, *lane 3*). In contrast, depletion of porin proteins had little effect on the PE level (Fig. 2, *A* and *B*). To further evaluate the impact of depletion of porin proteins on mitochondrial CL and PE synthesis, we took advantage of 4m (*psd2*Δ *dpl1*Δ *cho2*Δ *opi3*Δ) cells (14). In 4m cells, PE synthesis through the endosomal Psd2 and Dpl1-dependent CDP-ethanolamine pathways, and PE conversion to PC are blocked. Therefore, in synthetic medium supplemented with choline, 4m cells produce PE virtually only through Psd1 and the synthesized PE is not metabolized to PC. Logarithmically growing 4m and doxycycline-treated 4m *tet-POR* cells were labeled with [^{32}P]P$_i$ for 20 to 60 min in synthetic dextrose (SD) medium supplemented with 3 mM choline (SD + choline). The biosynthetic rates for all major phospholipids such as PC and PE in doxycycline-treated 4m *tet-POR* cells were lower than those for the corresponding phospholipids in 4m cells, probably because of a partial defect in cell growth; however, the biosynthetic rate of PE relative to that of PC in doxycycline-treated 4m *tet-POR* cells was almost identical with that in 4m cells (Fig. 2, *C* and *D*). In contrast, the biosynthetic rate of CL relative to that of PC in doxycycline-treated 4m *tet-POR* cells was ~5-fold lower than that in 4m cells (Fig. 2, *C* and *D*). These results suggested that the porin proteins Por1 and Por2 play a crucial role specifically in mitochondrial synthesis of CL, but not of PE, under these conditions.

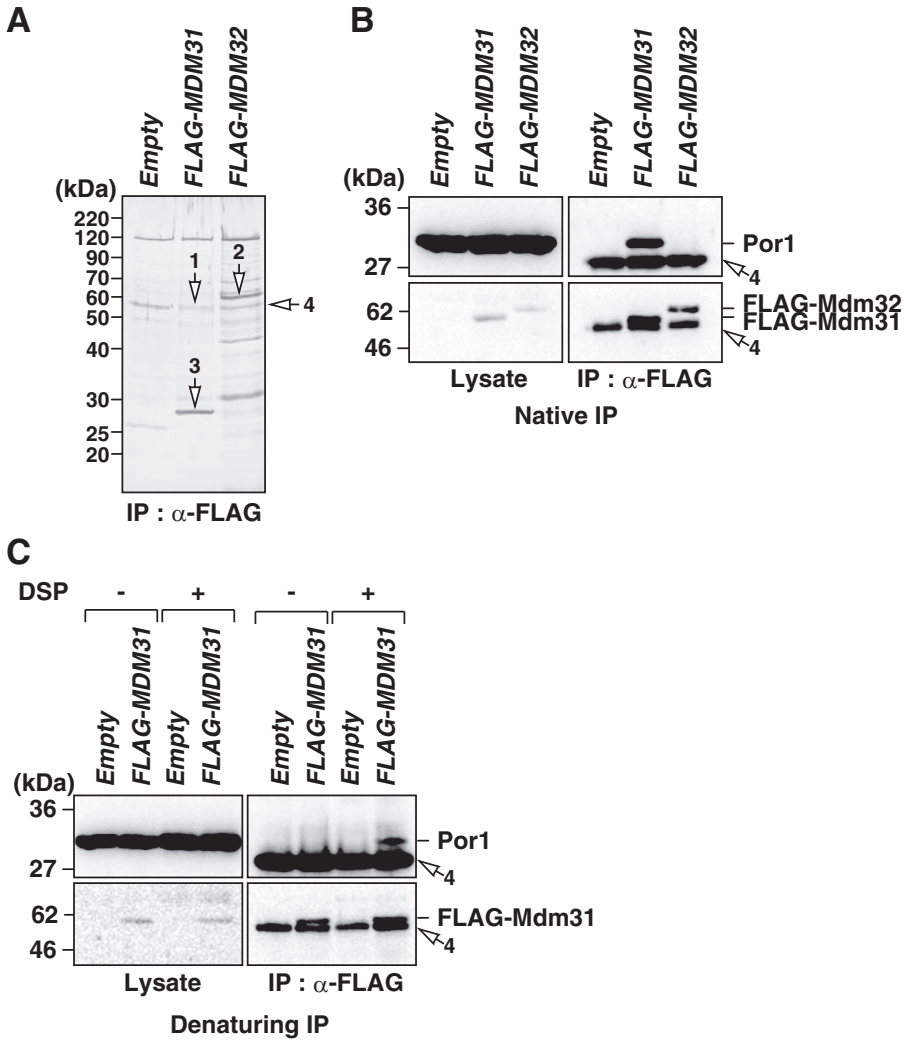

Figure 1. The outer membrane protein Por1 interacts with the inner membrane protein Mdm31. *A*, immunoprecipitation and MS reveal that Por1 interacts with Mdm31. Mitochondria (10 mg) from WT yeast cells carrying pRS424 (*Empty*), pRS424-*FLAG-MDM31* (*FLAG-MDM31*), or pRS424-*FLAG-MDM32* (*FLAG-MDM32*) were solubilized with 1% digitonin and then subjected to immunoprecipitation with anti-FLAG agarose. The immunoprecipitates were eluted with FLAG peptide, and analyzed by SDS-PAGE and silver staining. *B*, immunoprecipitation and immunoblotting show that Por1 interacts with Mdm31 but not Mdm32. Mitochondria (1 mg) from WT yeast cells carrying pRS424 (*Empty*), pRS424-*FLAG-MDM31* (*FLAG-MDM31*), or pRS424-*FLAG-MDM32* (*FLAG-MDM32*) were solubilized with 1% digitonin and then subjected to immunoprecipitation with anti-FLAG agarose. The immunoprecipitates were eluted with 2% SDS, and analyzed by immunoblotting with anti-FLAG and anti-Por1 antibodies. The *top panels* show immunoblots with anti-Por1 antibody. The *bottom panels* show immunoblots with anti-FLAG antibody. Blots on the *left side* show a lysate control omitting immunoprecipitation. *C*, cross-linking and immunoprecipitation show that Por1 interacts with Mdm31 in intact mitochondria. Mitochondria (0.5 mg) from yeast cells carrying pRS424 (*Empty*) or pRS424-*FLAG-MDM31* (*FLAG-MDM31*) were mock-treated (−) or cross-linked with 1 mM DSP (+), followed by solubilization and denaturation in buffer containing 1% SDS at 70 °C. The lysates were diluted with buffer containing 1% Triton X-100 and subjected to immunoprecipitation with anti-FLAG agarose. The immunoprecipitates were eluted with 2% SDS, reduced with 10% 2-mercaptoethanol, and then analyzed by immunoblotting as in *B*. *Arrows 1* and *2* indicate FLAG-Mdm31 and FLAG-Mdm32, respectively. *Arrow 3* indicates Por1 co-immunoprecipitated with FLAG-Mdm31. *Arrows 4* indicate the IgG that leaked from the anti-FLAG agarose and migrated similarly to FLAG-Mdm31.

Porin proteins are involved in both the Ups1-dependent and Ups1-independent CL accumulation pathways

CL synthesis in WT cells largely depends on Ups1 (17, 18), and as shown in Fig. 2, *A* and *B*, depletion of porin proteins led to a striking (~90%) decrease in the CL level as compared with that in WT cells. These observations suggested that porin proteins were involved in Ups1-dependent CL synthesis. However, as shown in Fig. 1, Por1 was found to interact with Mdm31, which, as well as Mdm32 and Fmp30, is required for the Ups1-independent CL accumulation that is enhanced under low mitochondrial PE conditions such as those in *ups2*Δ, *psd1*Δ, and *cho1*Δ cells (26). Therefore, we examined the effect of depletion of porin proteins on the Ups1-independent CL accumulation, namely, the CL level in *ups1*Δ *ups2*Δ cells. Deletion of *UPS1* reduced the CL level to ~20% of that in WT cells, and the CL level was largely restored on concomitant deletion of *UPS2* in *ups1*Δ cells (Fig. 3, *A* and *B*, *lanes 1–3*), thus being consistent with previous reports (17, 18, 26). Depletion of porin proteins in the *ups1*Δ *ups2*Δ background as well as the *UPS1 UPS2* background greatly reduced the CL level (Fig. 3, *A* and *B*, *lanes 6* and *7*). These results suggested that porin proteins are involved in both the Ups1-dependent and Ups1-independent CL accumulation pathways.

Porin proteins are required for the stability of Ups1 and Ups2

To determine whether or not depletion of porin proteins affects the molecular behavior of Ups1, the protein level of

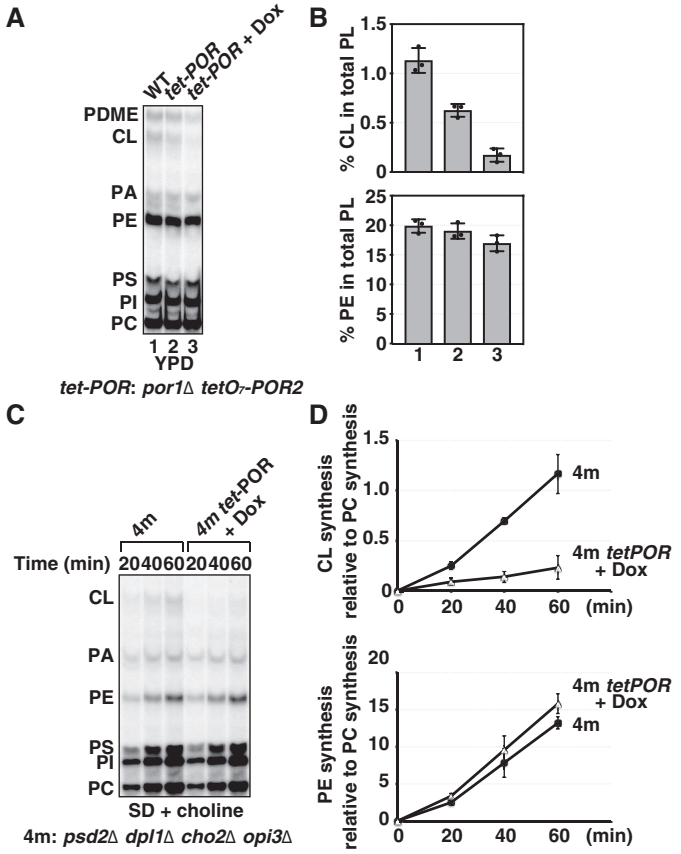

Figure 2. Depletion of porin proteins affects the CL level. *A* and *B*, depletion of porin proteins by suppressing *POR2* gene expression under *por1*Δ background strongly decreases CL level in yeast. WT (*lane 1*) and *por1*Δ *tetO*$_7$-*POR2* (*tet-POR*) (*lanes 2* and *3*) cells were cultured to saturation in YPD in the absence of doxycycline. The cells were diluted to A_{600} of 0.015 in YPD in the absence (*lanes 1* and *2*) or presence of 10 μg/ml doxycycline (+ Dox) (*lane 3*), and then further cultured in the presence of [^{32}P]P_i for 12 h. Total cellular phospholipids were extracted, and the ^{32}P radioactivities of the lipids were measured by scintillation counting. Lipids containing equivalent radioactivity were then subjected to TLC, and analyzed with an imaging analyzer. *B*, the percentages of CL (*upper panel*) and PE (*lower panel*) relative to the total major phospholipids (*PL*) (CL, PA, PE, PS, PI, and PC). The numbers at the *bottom of panels* correspond to the lane numbers in *A*. Values are mean ± S.D. (n = 3). *C* and *D*, depletion of porin proteins decreases CL synthesis but not PE synthesis in logarithmically growing cells. 4m (*psd2*Δ *dpl1*Δ *cho2*Δ *opi3*Δ) and 4m *por1*Δ *tetO*$_7$-*POR2* (4m *tet-POR*) cells were cultured to saturation in synthetic dextrose medium supplemented with 3 mM choline (SD + choline). Cells were diluted to A_{600} to 0.2 in SD + choline in the absence or presence of 20 μg/ml doxycycline (+ Dox), and further cultured for 8 h. Cells were then diluted to A_{600} to 1.0 in SD + choline in the absence or presence of 20 μg/ml doxycycline (+ Dox), and labeled with [^{32}P]P_i for 20, 40, and 60 min. At each time point, an equal aliquot of culture fluid was collected. After total lipid extraction and scintillation counting, lipids equivalent to 0.28 ml and 0.72 ml of cultures from 4m cells and doxycycline-treated 4m *tet-POR* cells (4m *tet-POR* + Dox), respectively, were loaded for TLC and analyzed as in Fig. 2*A*. *D*, the signal intensities of CL, PE, and PC were determined and expressed as values relative to the amount of PC at 60 min for each strain; the value for PC at 60 min was set as 100. Values are mean ± S.D. (n = 3). *Solid circle*, 4m cells; *open triangles*, 4m *tet-POR* + Dox.

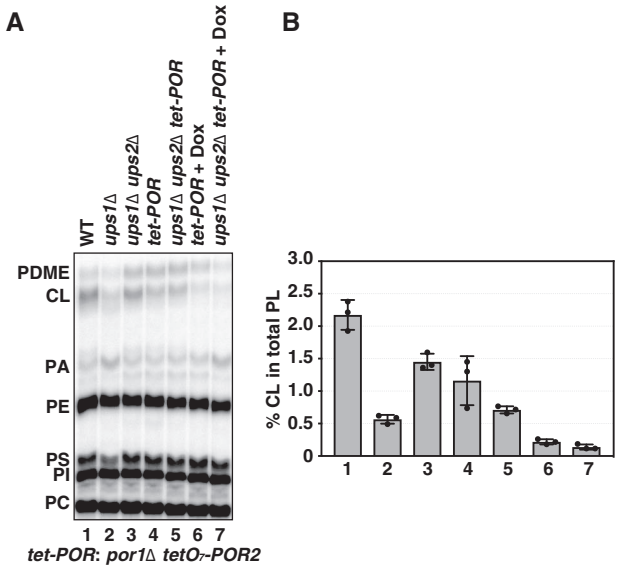

Figure 3. Porin proteins are required for Ups1-independent CL accumulation. *A* and *B*, depletion of porin proteins strongly decreases CL level in *ups1*Δ *ups2*Δ cells as well as in WT cells. WT (*lane 1*), *ups1*Δ (*lane 2*), *ups1*Δ *ups2*Δ (*lane 3*), *por1*Δ *tetO*$_7$-*POR2* (*tet-POR*) (*lanes 4* and *6*), and *ups1*Δ *ups2*Δ *por1*Δ *tetO*$_7$-*POR2* (*ups1*Δ *ups2*Δ *tet-POR*) (*lanes 5* and *7*) cells were cultured to saturation in YPD. The cells were diluted to A_{600} of 0.05 in YPD in the absence (*lanes 1–5*) or presence of 10 μg/ml doxycycline (*lanes 6* and *7*), and further cultured in the presence of [^{32}P]P_i for 16 h. Total cellular phospholipids were extracted and analyzed as in Fig. 2*A*. Values are mean ± S.D. (n = 3).

Ups1 in porin protein–depleted cells was analyzed by C-terminal tagging of the chromosomal *UPS1* gene with the 3xMYC epitope, followed by immunoblotting. The cellular level of Ups1 tagged with 3xMYC (Ups1–3xMYC) severely decreased in *tet-POR* (*por1*Δ *tetO*$_7$-*POR2*) cells even in the absence of doxycycline as compared with that in WT cells (Fig. 4*A*). In the presence of doxycycline, the Ups1–3xMYC level further decreased (Fig. 4*A*). Interestingly, we found that the cellular level of Ups2–3xMYC, examined as a control, decreased similarly to that of Ups1 in *tet-POR* cells (Fig. 4*B*). The reduction of the Ups1 and Ups2 levels seemed not to be because of the reduction in the CL level in *tet-POR* cells, because Ups1–3xMYC and Ups2–3xMYC did not decrease on deletion of *CRD1*, which encodes CL synthase (3, 4, 7) (Fig. 4, *A* and *B*). Inversely, Ups1–3xMYC increased in *crd1*Δ cells (Fig. 4*A*), implying feedback regulation of Ups1 expression in response to the CL level. These findings suggested that porin proteins are required for the maintenance of normal levels of Ups1 and Ups2.

It has been reported that a cofactor of Ups proteins, Mdm35, is required for efficient import to the IMS, and the stability of Ups1 and Ups2, which lack the conventional IMS-targeting signals (15, 16). The reductions of the Ups1 and Ups2 levels in porin protein–depleted cells were very similar to those observed in *mdm35*Δ cells (15, 16). Thus, we examined the cellular Mdm35 level by C-terminal tagging of the chromosomal *MDM35* gene with the 3xMYC epitope. The Mdm35–3xMYC level in *tet-POR* cells was also decreased as compared with that in WT cells (Fig. 4*C*). However, the reduction of the Mdm35–3xMYC level was moderate as compared with those of the Ups1–3MYC and Ups2–3xMYC levels. Furthermore, unlike Ups1–3xMYC and Ups2–3xMYC, the Mdm35–3xMYC level in *tet-POR* cells was not further decreased by doxycycline treatment (Fig. 4*C*). Thus, the strong reductions of the Ups1–3xMYC and Ups2–3xMYC levels in *tet-POR* cells treated with and without doxycycline does not seem to be merely because of the reduction of the Mdm35 level. Rather, the function of Mdm35 in stabilization of Ups1 and Ups2 seemed to be abrogated by depletion of porin proteins. Next, we investigated the physical interaction between Mdm35 and Por1. Mitochondria obtained from WT and *mdm35*Δ cells were treated with a

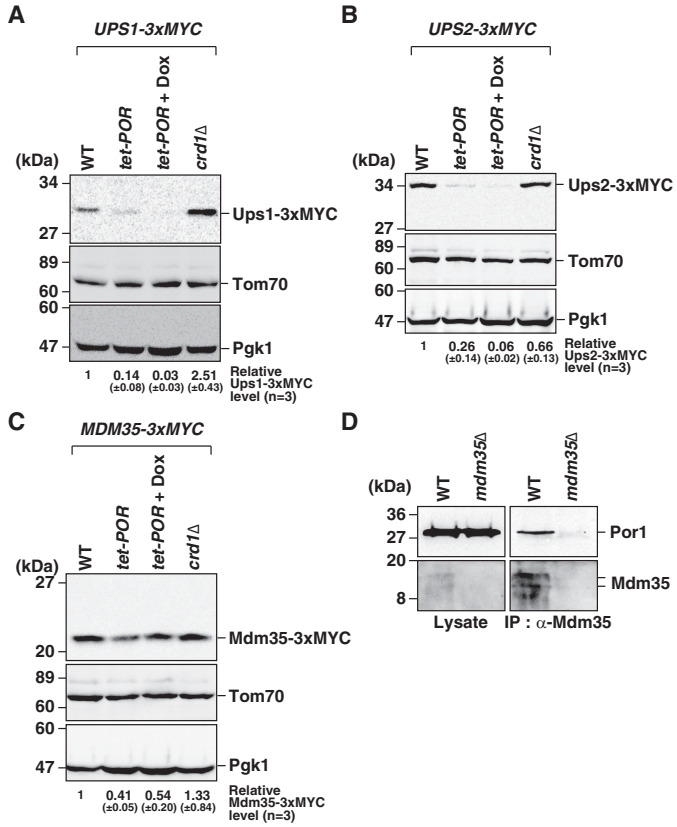

Figure 4. Porin proteins are required for the stabilities of Ups1 and Ups2, and interact with Mdm35. *A–C*, depletion of porin proteins strongly decreases the Ups1 and Ups2 levels. WT, *por1*Δ *tetO*$_7$*-POR2* (*tet-POR*), and *crd1*Δ cells expressing genomically tagged Ups1–3xMYC (*A*), Ups2–3xMYC (*B*), or Mdm35–3xMYC (*C*) were cultured to saturation in YPD in the absence of doxycycline. The yeast cells were diluted to A_{600} of 0.2 in YPD in the absence or presence of 10 μg/ml doxycycline (+ Dox), and further cultured for 8 h. After cultivation, cells were harvested, and analyzed by immunoblotting with antibodies against MYC tag (*top panel*), Tom70 (*middle panel*), and Pgk1 (*bottom panel*). The levels of Ups1–3xMYC (*A*), Ups2–3xMYC (*B*), and Mdm35–3xMYC (*C*) were quantified and normalized to Pgk1 levels. The relative levels of the 3xMYC-tagged proteins were shown at the *bottom*. The values for WT cells were set as 1. Values are mean ± S.D. (n = 3). *D*, immunoprecipitation and immunoblotting show that Por1 interacts with Mdm35. Mitochondria (2 mg) from WT or *mdm35*Δ cells were cross-linked with 1 mM DSP, solubilized with buffer containing 1% digitonin, and then subjected to immunoprecipitation with anti-Mdm35 antibodies. Immunoprecipitates were eluted with SDS-sample buffer containing 10% 2-mercaptoethanol and analyzed by immunoblotting with antibodies against Por1 (*top panel*) and Mdm35 (*bottom panel*).

chemical cross-linker, solubilized, and then subjected to immunoprecipitation with anti-Mdm35 antibodies. Por1 proteins in WT mitochondria, but not in *mdm35*Δ ones, were co-immunoprecipitated with anti-Mdm35 antibodies (Fig. 4*D*), demonstrating that Por1 specifically interacts with Mdm35. Taken together, these findings suggested that the interaction of porin proteins with Mdm35 is involved in the stabilization of Ups1 and Ups2.

Depletion of porin proteins affects Ups2-dependent PE synthesis in the post-diauxic phase

As shown in Fig. 4, depletion of porin proteins led to decreases in the protein levels of Ups1 and Ups2, raising the possibility that depletion of porin proteins affects Ups2-dependent PE synthesis, as well as CL synthesis. The PS transport by Ups2–Mdm35 for PE synthesis occurs specifically in respiration-active mitochondria such as those of yeasts in the post-diauxic phase, in which the yeasts consume all the glucose and shift their energy metabolism from glycolysis to oxidative phosphorylation (14). Upon cultivation in glucose medium, depletion of porin proteins did not affect PE synthesis of yeast cells in the log phase (Fig. 2); however, under these conditions the yeast cells only utilized glycolysis for energy production, *i.e.* not respiration, and therefore synthesized PE largely in a Ups2-independent manner. To precisely investigate the mitochondrial PE synthesis in porin protein– depleted cells, we again utilize 4m cells. Prior to analysis of phospholipid compositions, we investigated glucose consumption in 4m and 4m *tet-POR* cells in the absence or presence of doxycycline. As shown in Fig. S2, 4m and 4m *tet-POR* cells in the absence and presence of doxycycline consumed all the glucose in the medium after ~18-h cultivation. Accordingly, we analyzed the phospholipid compositions in 4m and porin protein– depleted 4m cells after 8-h cultivation (cells in the log phase) or 20-h cultivation (cells in the post-diauxic phase) in YPD medium. When cells were in the log phase, the PE level in doxycycline-treated 4m *tet-POR* cells was similar to those in 4m and doxycycline-untreated 4m *tet-POR* cells, whereas the CL level in doxycycline-treated 4m *tet-POR* cells was remarkably lower than those in 4m and doxycycline-untreated 4m *tet-POR* cells (Fig. 5, *A* and *B*, *lanes 1–3*), consistent with the data in Fig. 2. In contrast, when cells were in the post-diauxic phase, the PE level in doxycycline-treated 4m *tet-POR* cells was ~50% of those in 4m and doxycycline-untreated 4m *tet-POR* cells (Fig. 5, *A* and *B*, *lanes 4–6*). The reduction of the PE level in porin protein– depleted cells in the post-diauxic phase was very similar to that observed in *ups2*Δ cells (14). Next, we analyzed the phospholipid compositions of 4m and 4m *tet-POR* cells carrying the WT or null allele of the *UPS2* gene in the presence and absence of doxycycline in SD + choline medium. After 20-h cultivation, the PE level in doxycycline-treated 4m *tet-POR* cells was greatly decreased as compared with those in 4m and doxycycline-untreated 4m *tet-POR* cells (Fig. 5, *C* and *D*, *lanes 1–3*), but similar to that in 4m *ups2*Δ cells (Fig. 5, *C* and *D*, *lanes 3* and *4*). In addition, doxycycline treatment of 4m *ups2*Δ *tet-POR* cells did not greatly decrease the PE level as compared with those in 4m *ups2*Δ and doxycycline-untreated 4m *ups2*Δ *tet-POR* cells (Fig. 5, *C* and *D*, *lanes 4–6*). These results suggested that depletion of porin proteins affects PE metabolism specifically through abrogation of Ups2–Mdm35-mediated PS transfer in the post-diauxic phase.

The Por1 mutations, which decrease the interaction of Por1 with Mdm31 and Mdm35, affect CL synthesis

Porin proteins have a β-barrel fold, and most regions of them are embedded in the MOM. However, porin proteins contains nine short loop regions exposed to the IMS (27) (designated as L1 to L9, Fig. S3), which could interact with Mdm31 and Mdm35. To determine whether the loop regions are involved in the interactions with Mdm31 and Mdm35, the two or three amino acid residues in each IMS loop region of Por1, which are identical or similar to the corresponding amino acids in yeast Por2 or mouse VDAC1, were substituted with alanine (Fig. S3) (referred to as mut L1 to mut L9). Because L4 does not contain the amino acids conserved in yeast Por1, yeast Por2, and mouse

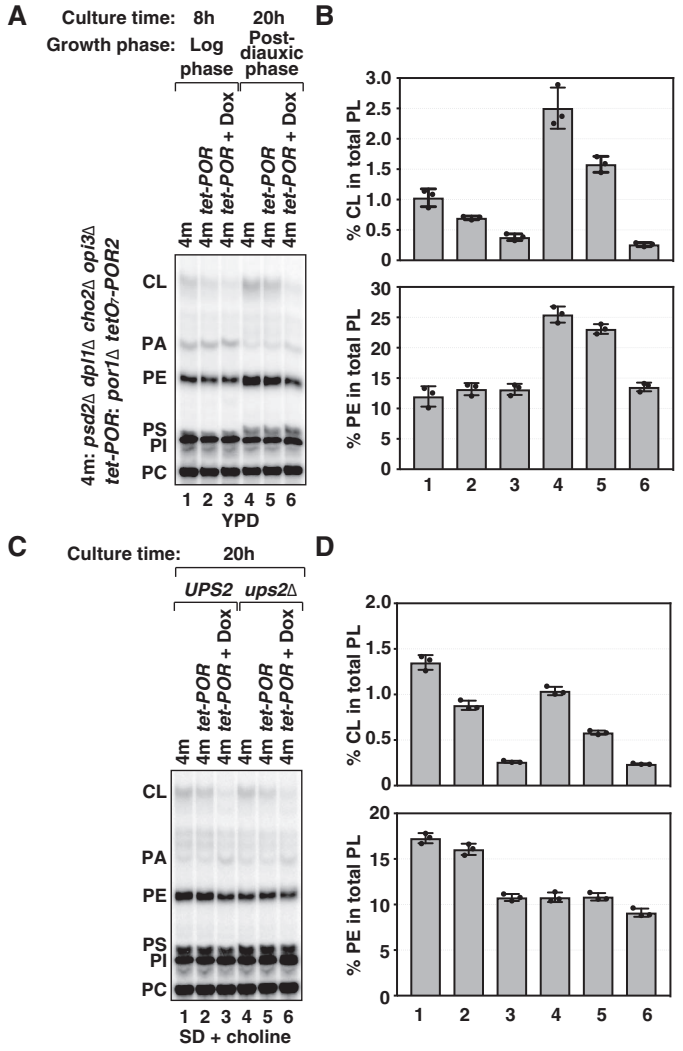

Figure 5. Depletion of porin proteins affects Ups2–Mdm35–dependent PE accumulation in the post-diauxic phase. *A* and *B*, depletion of porin proteins decreases PE level in cells in the post-diauxic phase but not in the log phase. 4m (*psd2*Δ *dpl1*Δ *cho2*Δ *opi3*Δ) (*lanes 1* and *4*) and 4m *por1*Δ *tetO*$_7$-*POR2* (4m *tet-POR*) (*lanes 2*, *3*, *5*, and *6*) cells were cultured to saturation in YPD in the absence of doxycycline. The cells were diluted to A_{600} of 0.05 in YPD in the absence (*lanes 1*, *2*, *4*, and *5*) or presence of 10 μg/ml doxycycline (+ Dox) (*lanes 3* and *6*), and further cultured in the presence of [^{32}P]P_i for 8 h (log phase) (*lanes 1–3*) or 20 h (post-diauxic phase) (*lanes 4–6*). Total cellular phospholipids were extracted and analyzed as in Fig. 2*A*. *B*, the percentages of CL and PE relative to the total major phospholipids (PL). The numbers at the *bottom* of the panel correspond to the lane numbers in *A*. Values are mean ± S.D. ($n = 3$). *C* and *D*, depletion of porin proteins decreases PE level in cells with WT *UPS2* gene but not in *ups2-null* cells. 4m (*lane 1*), 4m *tet-POR* (*lanes 2* and *3*), 4m *ups2*Δ (*lane 4*), and 4m *ups2*Δ *tet-POR* (*lanes 5* and *6*) were cultured to saturation in synthetic dextrose medium supplemented with 3 mM choline (SD + choline) in the absence of doxycycline. The cells were diluted to A_{600} of 0.05 in SD + choline in the absence (*lanes 1*, *2*, *4*, and *5*) or presence of 10 μg/ml doxycycline (+ Dox) (*lanes 3* and *6*), and further cultured in the presence of [^{32}P]P_i for 20 h. Total cellular phospholipids were extracted and analyzed as in Fig. 2*A*. *D*, the percentages of CL and PE relative to the total major phospholipids (PL). The numbers at the *bottom* of the panel correspond to the lane numbers in *A*. Values are mean ± S.D. ($n = 3$).

VDAC1, we excluded L4 from the analysis. Upon expression of the Por1 loop mutants in the *por1*Δ background by means of endogenous *POR1* promoter, the protein levels of the mutants varied according to the mutation. The level of mut L1 was slightly lower than that of WT Por1; mut L7, mut L8, and mut L9 exhibited severely decreased levels as compared with WT Por1; and the levels of mut L2, mut L3, mut L5, and mut L6 were similar to that of WT Por1 (Fig. 6*A*). Although *por1*Δ cells exhibit a growth defect in a nonfermentable ethanol/glycerol medium, as shown previously (28), expression of WT Por1 and all of the Por1 loop mutants facilitated the growth of *por1*Δ cells in the ethanol/glycerol medium (Fig. 6*B*), suggesting that these loop mutants still retained the fundamental functions of porin proteins, such as channel activity in the MOM. Next, we analyzed the interactions of Mdm31 or Mdm35 with five stable Por1 mutants (L1, L2, L3, L5, and L6), which exhibited protein levels comparable with that in WT Por1, by co-immunoprecipitation with FLAG-Mdm31 or -Mdm35. We evaluated binding affinities of Por1 variants to Mdm31 or Mdm35 through co-immunoprecipitation (co-IP) rates, namely, the ratio of protein level of Por1 variants in the immunoprecipitation fractions to that in the lysates. The co-IP rates of mut L1 with FLAG-Mdm31 and -Mdm35, respectively, were about 50 and 35% of those of WT Por1 with FLAG-Mdm31 and -Mdm35 (Fig. 6, *C–E*, *left panel*). In addition, the co-IP rate of mut L5 with Mdm35 was about 30% of that of WT Por1 with Mdm35 (Fig. 6, *D* and *E*, *left panel*), whereas the co-IP rate of mut L5 with FLAG-Mdm31 was comparable with that of WT Por1 with FLAG-Mdm31 (Fig. 6, *C* and *E*, *left panel*). Unexpectedly, it was found that the co-IP rate of mut L6 with FLAG-Mdm31 and -Mdm35, respectively, were 5- and 8-fold of those of WT Por1 with FLAG-Mdm31 and Mdm35 (Fig. 6, *C–E*, *right panel*). From these results, we concluded that the L1 region is important for the interaction of Por1 with both Mdm31 and Mdm35, and that the L5 region is involved in the interaction of Por1 with Mdm35, but not with Mdm31. These conclusions were also obtained when the binding affinities were evaluated through the amounts of Por1 variants co-precipitated with FLAG-Mdm31 or -Mdm35 relative to those of FLAG-Mdm31 or -Mdm35 in immunoprecipitation fractions (Fig. S4).

Finally, the CL levels in *tet-POR* cells expressing the five stable Por1 mutants and an unstable Por1 mutant, mut L8, in the presence of doxycycline were analyzed. The CL levels in the cells expressing mut L1 and mut L5, respectively, were significantly decreased by ~50 and ~20% as compared with those in cells expressing WT Por1, whereas the CL levels in the cells expressing mut L2, mut L3, mut L6, and mut L8 were not significantly affected (Fig. 6, *F* and *G*). The decrease in the CL level in the cells expressing mut L1 is not likely because of the decreased protein stability of mut L1, because mut L8, which is more unstable than mut L1, can increase the CL level in doxycycline-treated *tet-POR* cells to the same extent as WT Por1. These results suggested a correlation between the abilities of Por1 variants to interact with Mdm31/Mdm35 and to complement the defect in CL biosynthesis of porin protein–depleted cells. This supported the notion that interactions of porin proteins with Mdm31 and Mdm35 are essential for maintenance of a normal CL level. Importantly, mut L1 and mut L5 were fully capable of supporting the respiratory growth of *por1*Δ cells (Fig. 6*B*), suggesting that the decreases in the CL level observed in the cells expressing mut L1 and mut L5 were not indirect effects of perturbation of general mitochondrial integrity or cellular energy metabolism in porin protein–deficient cells. Taken

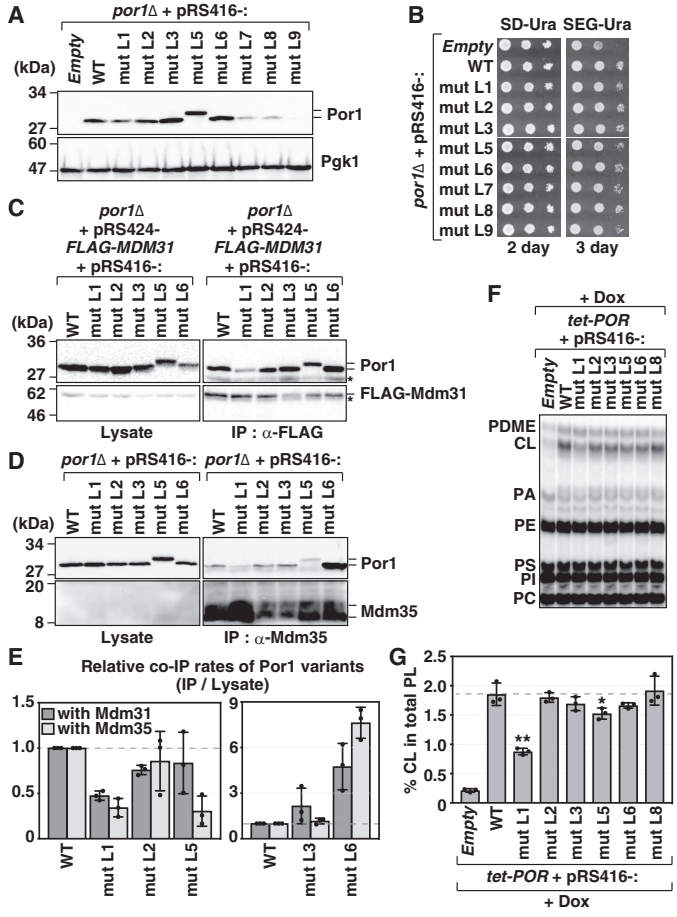

Figure 6. Identification of the IMS-loop regions of Por1 required for interaction with Mdm31 and Mdm35. *A*, expression levels of WT Por1 and Por1 loop mutants. *por1*Δ cells carrying pRS416 (*Empty*), pRS416-*POR1* (WT), or pRS416 encoding Por1 loop mutants, as indicated (initial A_{600}, 0.05), were grown in SD-URA for 16 h. Total protein extracts from the cells were subjected to immunoblotting with anti-Por1 (*top panel*) and anti-Pgk1 (*bottom panel*) antibodies. Por1 mut L5 migrates slower than WT Por1 and the other Por1 loop mutants because of the amino acid substitutions. *B*, Por1 loop mutants can rescue the growth defect of *por1*Δ cells in nonfermentable carbon sources. *por1*Δ cells carrying pRS416 (*Empty*), pRS416-*POR1* (WT), or pRS416 encoding Por1 loop mutants, as indicated, were serially diluted and spotted onto synthetic dextrose (fermentable carbon source) medium lacking uracil (SD-URA) or synthetic ethanol/glycerol (nonfermentable carbon sources) medium lacking uracil (SEG-URA) plates and incubated for 2 days (SD-URA) or 3 days (SEG-URA). *C* and *E*, mutation to the loop 1 of Por1 (Mut L1) decreases the interaction of Por1 with Mdm31. Mitochondria (0.5 mg) from *por1*Δ cells carrying pRS424-*FLAG-MDM31* and pRS416-*POR1* (WT) or pRS416 encoding Por1 loop mutants, as indicated, were solubilized with 1% digitonin and then subjected to immunoprecipitation with anti-FLAG agarose. The immunoprecipitates were eluted with 2% SDS and analyzed by immunoblotting with anti-Por1 (*top panel*) and anti-FLAG (bottom panel) antibodies. *Asterisks* indicate IgG from anti-FLAG agarose. *D* and *E*, mutation to the loop 1 or 5 of Por1 (Mut L1 or Mut L5) decreases the interaction of Por1 with Mdm35. Mitochondria (1 mg) from *por1*Δ cells carrying pRS416-*POR1* (WT) or pRS416 encoding Por1 loop mutants, as indicated, were cross-linked with 1 mM DSP, solubilized with buffer containing 1% digitonin, and then subjected to immunoprecipitation with anti-Mdm35 antibodies. Immunoprecipitates were eluted with SDS-sample buffer containing 10% 2-mercaptoethanol, and then analyzed by immunoblotting with anti-Por1 (*top panel*) and anti-Mdm35 (*bottom panel*) antibodies. Mdm35 was not detected in the Lysate fraction because of low protein abundance. *E*, the intensities of Por1 variants in Lysate and IP fractions in *C* and *D* were measured. The co-immunoprecipitation rates (IP/Lysate) of Por1 variants with FLAG-Mdm31 and Mdm35 relative to that of WT Por1 were plotted. The value for WT Por1 was set as 1. Values are mean ± S.D. ($n = 3$). *F* and *G*, the CL levels in the cells expressing mut L1 or mut L5 were lower than that in cells expressing WT Por1. *por1*Δ *tetO*$_7$-*POR2* (*tet-POR1*) cells carrying pRS416 (*Empty*), pRS416-*POR1* (WT), or pRS416 encoding Por1 loop mutants, as indicated, were cultured to saturation in SD-URA in the absence of doxycycline. The cells were diluted to A_{600} of 0.05 in YPD in the presence of 10 μg/ml doxycycline (+ Dox), and further cultured in the presence of [^{32}P]P_i for 16 h. Total cellular phospholipids were extracted and analyzed as in Fig. 2*A*. Values are mean ± S.D. ($n = 3$). *, $p < 0.05$ and **, $p < 0.01$ *versus* the corresponding value for WT Por1.

together, these findings suggested that porin proteins have novel functions in mitochondrial phospholipid synthesis.

Function of porin proteins in CL metabolism is evolutionally conserved

Porin proteins are highly conserved throughout eukaryotes and bacteria. Three porin proteins, VDAC1, VDAC2, and VDAC3, exist in mammals (29). We next investigated whether or not the function of porin proteins in mitochondrial phospholipid homeostasis observed in yeast is common among eukaryotes. *VDAC1* from mouse (*MmVDAC1*) was introduced into *tet-POR* cells and then the phospholipid composition was analyzed. Introduction of *MmVDAC1* restored the CL level in *tet-POR* cells in the presence of doxycycline (Fig. 7, *A* and *B*), demonstrating that mammalian VDAC1 can functionally substitute for yeast porin proteins with regard to CL metabolism. Next, we analyzed the phospholipid composition in HeLa cells upon knockdown of *VDAC1* and *VDAC2* (Fig. 7, *C–E*). Unlike in yeast, phosphatidylglycerol (PG), an intermediate of the CL synthetic pathway, was discernible in HeLa cells (Fig. 7*D*). Concomitant knockdown of *VDAC1* and *VDAC2* significantly reduced the CL and PG levels (Fig. 7, *D* and *E*), but not the levels of the other phospholipids (Fig. S5). These findings suggested that the function of porin proteins in maintenance of the CL level has been evolutionally conserved.

Discussion

In the present study, we identified a yeast porin protein, Por1 as a protein interacting with the MIM protein Mdm31 (Fig. 1) that is required for Ups1-independent and low mitochondrial PE-enhanced accumulation of CL (26). In addition, we found that Por1 also interacts with the IMS protein Mdm35 (Fig. 4*D*) that forms protein complexes with Ups1 and Ups2, which function as PA and PS transfer proteins, respectively. Depletion of porin proteins Por1 and Por2 by doxycycline-treatment of *por1*Δ *tetO*$_7$-*POR2* (*tet-POR*) cells led to destabilization of Ups1 and Ups2 (Fig. 4, *A* and *B*), defects in Ups1-dependent and Ups1-independent CL accumulation (Figs. 2 and 3), and loss of Ups2-dependent PE synthesis (Fig. 5), such as PE synthesis enhanced in yeast cells at the post-diauxic phase. However, depletion of the porin proteins did not affect Ups2-independent mitochondrial PE synthesis such as mitochondrial PE synthesis in 4m cells at the logarithmic growth phase (Fig. 2, *C* and *D*). Moreover, Por1 mutations (mut L1 and mut L5) that weakened the interactions of Por1 with Mdm31 and Mdm35 (Fig. 6, *C–E*) were shown to reduce Por1 activity to complement the CL biosynthetic defect of porin protein–depleted cells (Fig. 6, *F* and *G*), even though the mutations did not affect the Por1 function required for cell growth in a nonfermentable ethanol/glycerol medium (Fig. 6*B*). These results demonstrated that the yeast porin proteins Por1 and Por2 have specific functions in mitochondrial phospholipid metabolism.

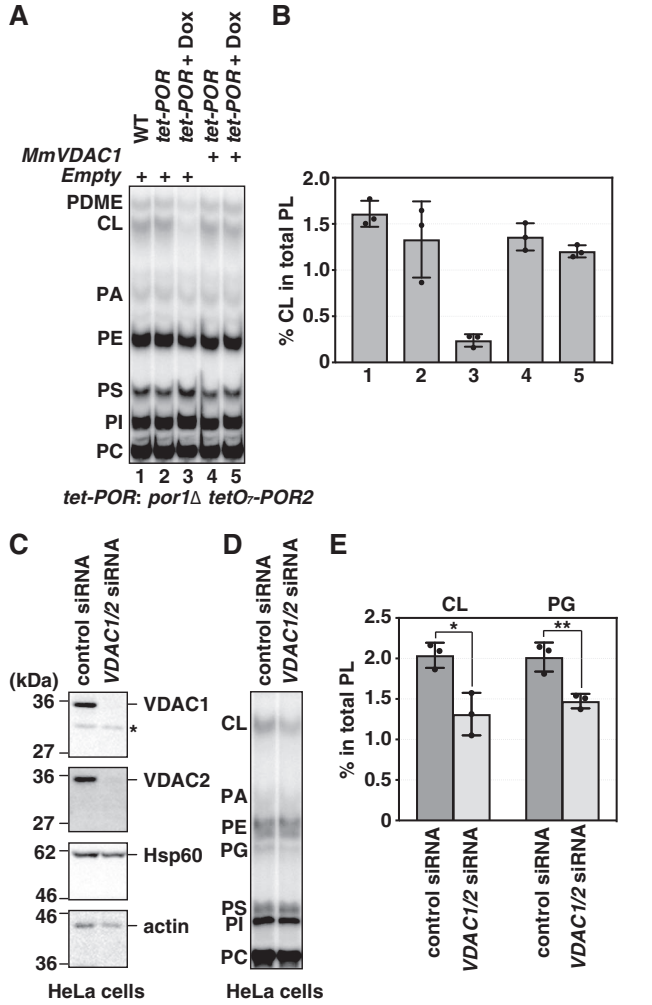

Figure 7. Mammalian VDACs are involved in CL accumulation. *A* and *B*, mouse *VDAC1* (*MmVDAC1*) can complement the defect in CL accumulation of porin protein–depleted cells. WT (*lane 1*) and *por1*Δ *tetO*$_7$*-POR2* (*tet-POR1*) (*lanes 2–5*) cells carrying pRS416TA2 (*Empty*) (*lanes 1–3*) or pRS416TA2–*MmVDAC1* (*MmVDAC1*) (*lanes 4* and *5*), which expresses *MmVDAC1* under the control of the *TEF* promoter, were cultured to saturation in SD-URA. The yeast cells were diluted to A_{600} of 0.05 in YPD in the absence (*lanes 1*, *2*, and *4*) or presence of 10 μg/ml doxycycline (+ Dox) (*lanes 3* and *5*), and further cultured in the presence of [^{32}P]P_i for 16 h. Total cellular phospholipids were extracted and analyzed as in Fig. 2*A*. Values are mean ± S.D. (n = 3). *C–E*, concomitant knockdown of *VDAC1* and *VDAC2* decreases CL level in HeLa cells. HeLa cells were transfected with control siRNA or siRNAs against both *VDAC1* and *VDAC2* three times. *C*, after siRNA transfection, cells were harvested and analyzed by immunoblotting with antibodies against VDAC1, VDAC2, Hsp60, and actin. *Asterisk* indicates nonspecific bands. *D* and *E*, siRNA-treated HeLa cells were incubated with [^{32}P]P_i for 24 h. Total cellular phospholipids were extracted and analyzed as in Fig. 2*A*. *E*, the percentages of CL and PG relative to the total major phospholipids (PL) (CL, PA, PE, PG, PI, and PC). Values are mean ± S.D. (n = 3). *, $p < 0.03$ and **, $p < 0.01$.

Por1 forms a solute-conducting channel and is largely responsible for the permeability of the MOM (23). Accordingly, there is a possibility that the defect in CL synthesis of porin protein–depleted cells could be because of decreased concentrations of metabolites such as CTP, which is required for CL biosynthesis (8). However, we believe that this is not the case because of the following: (i) Por2 is incapable of forming a channel and conferring permeability to the outer membrane (22, 23). Nevertheless, Por2 apparently acts redundantly with Por1 in maintenance of the CL level (Fig. 2, *A* and *B*). (ii) Por1 carrying mutations that significantly affect CL accumulation was able to fully support respiratory growth of yeast cells (Fig. 6*B*). Thus, the function of Por1 in maintenance of the CL level seems to be independent of its basal functions such as channel activity. (iii) Even *por1*Δ *por2*Δ double-knockout cells are able to retain mitochondrial DNA and grow under nonfermentable conditions (23), although null mutants as to nucleotide carriers of the MIM such as AAC2 (ATP/ADP carrier) and Rim2 (pyrimidine nucleotide carrier) are unable to grow under nonfermentable conditions (30, 31). Therefore, nucleotides could be imported into mitochondria to a certain degree in the absence of porin proteins. Regarding this, it was reported that the TOM translocon channel substitutes for the Por1 channel in *por1*Δ cells (32).

The early steps of the CL accumulation pathway include Ups1-dependent and Ups1-independent ones (17, 18). In the present study, we found that depletion of porin proteins leads to defects in both the Ups1-dependent and Ups1-independent CL accumulation pathways (Fig. 3), and that Por1 binds with Mdm31 and Mdm35, which are required for each of those pathways. Therefore, binding of Mdm31 and Mdm35, respectively, to porin proteins seemed to be essential for the Ups1-independent and Ups1-dependent CL accumulation.

Systemic mutation analysis of loop regions of Por1 exposed to the IMS side revealed that the L1 region is important for interaction with both Mdm31 and Mdm35, and the L5 region is important for interaction with Mdm31 but not with Mdm35 (Fig. 6). These findings suggested overlapping but partially distinct binding sites for Mdm31 and Mdm35. Accordingly, binding of Mdm31 and Mdm35 to Por1 could be mutually competitive. This might be relevant as to the reciprocal regulation of the Ups1-dependent and Ups1-independent CL accumulation pathways.

How does binding of the porin proteins to Mdm31 function in the Ups1-independent CL accumulation pathway (Fig. 8*A*)? One possible explanation is that binding of the MOM proteins, porins, and the MIM protein Mdm31 might induce the proximity of the MOM and MIM, facilitating the transfer of PA required for CL synthesis, from the MOM to the MIM. The second possibility is that interaction of porin proteins and Mdm31 leads to the formation of a large protein complex including Fmp30 that exhibits homology to mammalian NAPE-specific phospholipase D, facilitating the supply of phospholipid substrate to the enzyme Fmp30 from the MOM. The substrates of Fmp30 remain to be established, but analyses of Fmp30 with point mutations have revealed that the hydrolase activity of Fmp30 is required for its function (33). It is also noteworthy that physical interactions of Fmp30 with Mdm31 and Mdm32 were revealed previously (26). Moreover, interaction of porin proteins and Mdm31 might trigger the Mdm31, Mdm32, or Fmp30 function. To address these issues, we are currently attempting clarification of the substrate and product of the enzyme Fmp30.

The next question is what is the function of binding of porin proteins to Mdm35? Ups1 and Ups2 are imported into the IMS through the translocase of the outer membrane (TOM) complex via interaction with Mdm35 (15, 16). Interaction of Ups1 and Ups2 with Mdm35 also protects Ups1 and Ups2 against intramitochondrial proteolysis by inner membrane proteases

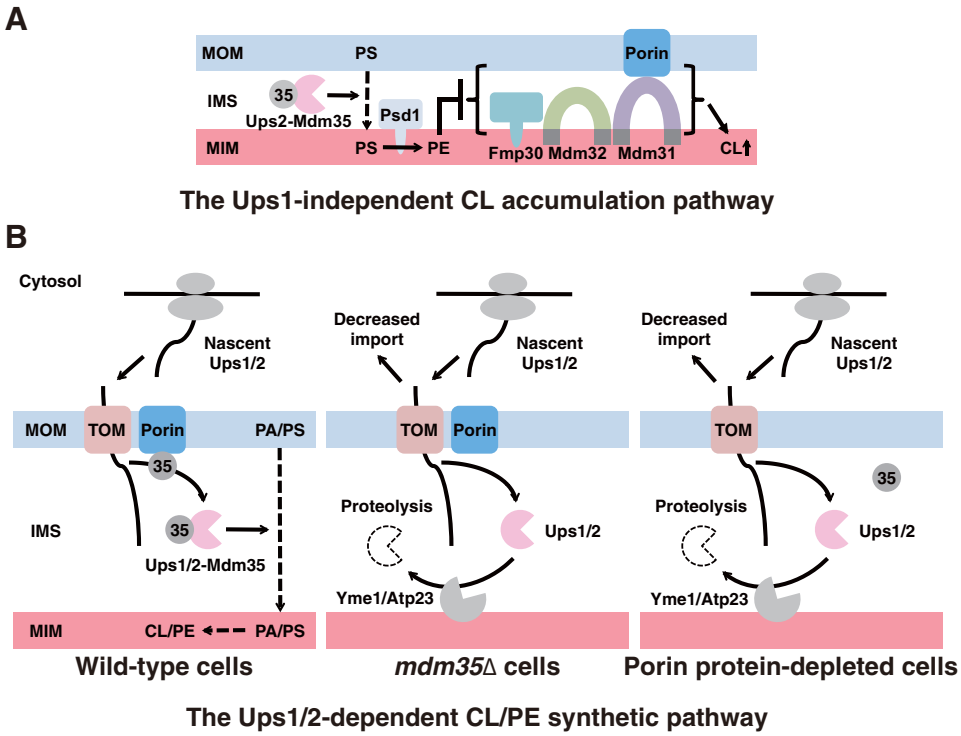

Figure 8. Schematic models of the functions of porin proteins in mitochondrial phospholipid metabolism. Porin proteins integrate mitochondrial phospholipid metabolism through two distinct functions as follows. *A*, porin proteins function in the Ups1-independent CL accumulation. Porin proteins directly or indirectly interact with the MIM protein Mdm31. The interaction is prerequisite for the Ups1-independent CL accumulation pathway involving Fmp30, Mdm31, and Mdm32. The pathway is inhibited by mitochondrial PE under normal conditions, and activated under low mitochondrial PE conditions such as in *ups2*Δ or *psd1*Δ cells. *35* designates Mdm35. *B*, porin proteins function in the Ups1-dependent CL synthesis and Ups2-dependent PE synthesis. Porin proteins directly or indirectly interact with Mdm35 (designated as *35*), and are required for the function of Mdm35 in efficient import and stabilization of Ups1 and Ups2 in the IMS (*left panel*). In the absence of Mdm35 (*center panel*) or porin proteins (*right panel*), the Ups1 and Ups2 levels are severely reduced because of the decreased import and the intramitochondrial proteolysis.

such as Yme1 and Atp23. Depletion of porin proteins led to destabilization of Ups1 and Ups2 (Fig. 4, *A* and *B*), similarly to deletion of *MDM35* (15, 16), and affected the Ups1-dependent CL accumulation (Figs. 2 and 3) and the Ups2-dependent PE accumulation (Fig. 5). These findings suggest that binding of porin proteins to Mdm35 is required for Mdm35 functions in import and stabilization of Ups1 and Ups2 (Fig. 8*B*). Thus, we speculate that porin proteins would facilitate the formation of a functional complex of Mdm35 and nascent Ups proteins that are translocated through the TOM complex.

Porin proteins are highly conserved from bacteria to eukaryotic cells. Mammals have three porin proteins, VDAC1, VDAC2, and VDAC3. Expression of VDAC1 in porin protein–depleted yeast cells restored the CL level. Furthermore, double knockdown of *VDAC1* and *VDAC2* led to a decrease in the CL level in HeLa cells (Fig. 7). These findings suggested that the function of porin proteins in phospholipid metabolism is conserved throughout eukaryotic cells. Preli, Slmo2, and Triap1 are mammalian homologs of Ups1, Ups2, and Mdm35, respectively, and can functionally substitute for their counterparts in yeast (13, 34), whereas Mdm31 and Mdm32 homologs are only found in fungi. Thus, VDACs could function in phospholipid metabolism in mammals through regulation of the Preli-Triap1 and Slmo2-Triap1 complexes. In addition, there is a possibility that a functional counterpart of Mdm31 exists in mammals and binds to VDACs. Determining the interactome of mammalian VDACs will help solve this issue in the future.

In conclusion, we revealed the novel functions of porin proteins in mitochondrial phospholipid metabolism. The new role of an old player will provide a framework for understanding the mitochondrial phospholipid metabolism universally conserved among species.

Experimental procedures

Yeast strains

The yeast strains used in this study are listed in Table S1. Complete disruption, promoter replacement, and tagging of the yeast genes were accomplished by PCR-mediated gene replacement (35) with a pair of primers and a template plasmid, as shown in Table S2.

Plasmids

Plasmid pRS424-*FLAG-MDM31* encoding FLAG-tagged Mdm31 was constructed as follows. A DNA fragment encoding Mdm31 tagged with a FLAG epitope at near the N terminus was constructed by PCR overlap extension recombination, using two pairs of primers (M13 rev primer (5′-CAGGAAACAGCTATGAC-3′) and FLAG-MDM31-R primer (5′-TGTCATCGTCATCCTTGTAATCCTCATTAGAATATGCTCTTAGC-3′), and FLAG-MDM31-F primer (5′-TACAAGGATGACGATGACAAGTCTAAAACTGGAAGGGATG-3′) and MDM31-R2 primer (5′-TCAATTGCGGTAGATCG-3′)), and a template plasmid, pRS424-MDM31, encoding Mdm31 (20) (gift from Y. Tamura). The resulting fragment was digested with

NotI and HpaI and then ligated with a large DNA fragment of pRS424-MDM31 digested with NotI and HpaI.

Plasmid pRS424-*FLAG-MDM32* encoding FLAG-tagged Mdm32 was constructed as follows. A DNA fragment encoding Mdm32 tagged with a FLAG epitope near the N terminus was constructed by PCR overlap extension recombination, using two pairs of primers (M13 rev primer (5′-CAGGAAACAGCTATGAC-3′) and FLAG-MDM32-R primer (5′-TGTCATCGTCATCCTTGTAATCAGCCTTGGTAGTGAAC-3′), and FLAG-MDM32-F primer (5′-TACAAGGATGACGATGACAAGTCCAATATTGAGACTATTTTGC-3′) and MDM32-R2 primer (5′-CCGTGAAATCAAACTTCG-3′)), and a template plasmid, pRS424-MDM32, encoding Mdm32 (20) (gift from Y. Tamura). The resulting fragment was digested with NotI and HpaI, and then ligated with a large DNA fragment of pRS424-MDM32 digested with NotI and HpaI.

Plasmid pRS416-*POR1* was constructed as follows. The *POR1* ORF flanked by the native *POR1* promoter and terminator (genomic regions 795 bp upstream and 586 bp downstream of the *POR1* locus) (36) was amplified by PCR with a primer set, POR1BamHI-F (ATGCGGATCCGCTGATGAAGCAGGTGTTGTTGTCT) and POR1NotI-R (AGTCGCGGCCGCGAATATCAAAGCTTCCTGGAGTCAGAAAAG). The resulting fragment was digested with BamHI and NotI, and then ligated with a large DNA fragment of pRS416 digested with BamHI and NotI.

To construct pRS416-*POR1* harboring mutations in each loop region exposed to the IMS as shown in Fig. S3, DNA fragments encoding the *POR1* loop mutants were amplified by PCR overlap extension recombination, using the pRS416-*POR1* plasmid as the template, primers POR1BamHI-F (ATGCGGATCCGCTGATGAAGCAGGTGTTGTTGTCT) and POR1NotI-R (AGTCGCGGCCGCGAATATCAAAGCTTCCTGGAGTCAGAAAAG), and the primers listed as follows: Mut L1-F, ATGTGCAAACAACAACCGCCGCTGCCATTAAGTTCTCATTGAAGG; Mut L1-R, CCTTCAATGAGAACTTAATGGCAGCGGCGGTTGTTGTTTGCACAT; Mut L2-F, CGTGGAAGCAAAGTTGAATGCCGCTCAAACCGGCTTGGGTCTAAC; Mut L2-R, GTTAGACCCAAGCCGGTTTGAGCGGCATTCAACTTTGCTTCCACG; Mut L3-F, CCAAATTAGAGTTTGCCAACGCTACCGCTGCTCTAAAGAACGAATTGATCA; Mut L3-R, TGATCAATTCGTTCTTTAGAGCAGCGGTAGCGTTGGCAAACTCTAATTTGG; Mut L5-F, TTGGTGACTTAACTATGGCCGCCGCAGCTATTGTTGGTGGCGCAGAGT; Mut L5-R, ACTCTGCGCCACCAACAATAGCTGCGGCGGCCATAGTTAAGTCACCAA; Mut L6-F, TGGCTTTAAGTTATTTCGCCGCAGCCGCCTCCTTGGGCGCTACATTGA; Mut L6-R, TCAATGTAGCGCCCAAGGAGGCGGCTGCGGCGAAATAACTTAAAGCCA; Mut L7-F, TTGACTTCTTCCAAAACGTCGCCGCCGCTGCACAGGTCGGTGCTAAGGCTA; Mut L7-R, TAGCCTTAGCACCGACCTGTGCAGCGGCGGCGACGTTTTGGAAGAAGTCAA; Mut L8-F, AATTCGCCACTAGATATTTGGCTGCTGCATCTGCCCAAGTTAAGGCTAAGGTG; Mut L8-R, CACCTTAGCCTTAACTTGGGCAGATGCAGCAGCCAAATATCTAGTGGCGAATT; Mut L9-F, TGGCTTACAAGCAATTGTTAGCAGCTGCCGTCACTCTGGGTGTCGGTT; Mut L9-R, AACCGACACCCAGAGTGACGGCAGCTGCTAACAATTGCTTGTAAGCCA. The resulting fragment was digested with BamHI and NotI, and then ligated with a large DNA fragment of pRS416 digested with BamHI and NotI.

Plasmids pRS416TA and pRS416TA2 carrying the *TEF* promoter, multiple cloning sites, and the *ADH1* terminator were constructed as follows. Plasmid pFA6a-*natNT2* carrying the *ADH1* terminator (37) was digested with MfeI, followed by blunt-ending of the 5′-protruding termini with DNA polymerase I (Klenow fragment), and then digestion with XhoI. The digested DNA fragment containing the *ADH1* terminator was cloned into pRS416 digested with XhoI and NaeI, which produced blunt ends. The resultant plasmid was digested with BstX1, followed by blunt-ending of the 3′-protruding termini with T4 DNA polymerase I, and then digestion with SacI. The digested DNA large fragment was ligated with the DNA fragment carrying the *TEF* promoter, which was obtained by digestion of pYM-N18 (37) carrying the *TEF* promoter with XbaI, followed by blunt-ending of the 5′-protruding termini with T4 DNA polymerase, and then digestion with SacI. The resultant plasmid was named pRS416TA. For construction of pRS416TA2, which is smaller than pRS416TA, pRS416TA was digested with SacI and PvuII, followed by blunt-ending of the 3′-protruding termini with T4 DNA polymerase. The resultant large DNA fragment was self-ligated to produce pRS416TA2.

Mouse *VDAC1* (*MmVDAC1*) was cloned into pRS416TA2 by yeast homologous recombination. Mouse *VDAC1* was amplified by RT-PCR with a primer set, GTGGCGGCCGCTCTAGAACTAGTGGATCCCCCGGGCTGCAATGGCCGTGCCTCCCACATACGCCG and ATAAATCATAAGAAATTCGCCTCGAGGTCGACGGTATCGATTATGCTTGAAATTCCAGTCCTAGG. *tet-POR* cells were transformed with the amplified *MmVDAC1* gene, and the plasmid linearized with EcoRI and HindIII.

Cell culture

Yeast cells were grown at 30 °C in YPD (1% yeast extract, 2% peptone, 0.008% adenine, and 2% glucose), SD + choline (0.67% yeast nitrogen base without amino acids, 0.2% drop out mix complete amino acids, 0.008% adenine, 2% glucose, and 3 mM choline, pH 6.0), SD-URA (0.67% yeast nitrogen base without amino acids, 0.2% drop out mix lacking uracil, 0.008% adenine, and 2% glucose, pH 6.0), SEG-URA (0.67% yeast nitrogen base without amino acids, 0.2% drop out mix lacking uracil, 0.008% adenine, 3% ethanol, and 3% glycerol, pH 6.0), or SD-TRP (0.67% yeast nitrogen base without amino acids, 0.2% drop out mix lacking tryptophan, 0.008% adenine, and 2% glucose, pH 6.0). Doxycycline (Sigma-Aldrich) was used at 10 or 20 μg/ml as stated to suppress $tetO_7$ promoter activity. HeLa cells were cultured in DMEM (Gibco Laboratories) supplemented with 10% fetal bovine serum under 5% CO_2–95% air at 37 °C.

siRNA transfection

HeLa cells were transfected with control siRNA (Ambion) or concomitantly with *VDAC1* siRNA (sense 5′-GAAUACCGACAAUACACUAtt-3′ and antisense 5′-UAGUGUAUUGUCGGUAUUCca-3′) (Ambion) and *VDAC2* siRNA (sense, 5′-AACUGGAUGUGAAAACAAAtt-3′ and antisense, 5′-UUU-

GUUUUCACAUCCAGUUtc-3′) (Ambion) with RNAiMAX Reagent (Invitrogen) three times at 24-h intervals.

Analysis of cellular phospholipid compositions

Yeast cells were cultured at 30 °C overnight in the medium indicated. The cells were then diluted as indicated in either the absence or presence of 10 μg/ml doxycycline, and then further incubated at 30 °C for different periods in the presence of 1 μCi/ml of [^{32}P]Pi. After incubation, the cells were harvested, resuspended in 150 μl of 80% ethanol, and then kept at −80 °C until all samples had been collected. The samples were heated at 95 °C for 15 min, mixed with 800 μl of chloroform/methanol (1:1, v/v), and then vortexed. 330 μl of 0.1 M HCl/0.1 M KCl was then added to the samples. The organic phase was obtained by centrifugation at 3000 × *g* for 2 min. Samples containing equivalent radioactivity were collected and then dried in a centrifugal evaporator and dissolved in chloroform/methanol (1:2, v/v). The samples were then subjected to TLC on a TLC plate (Macherey-Nagel) which had been pretreated with 1.8% boric acid, with the solvent system of chloroform/ethanol/water/triethylamine (30:30:5:35, v/v) (38). ^{32}P-labeled phospholipids were detected and quantitated with an imaging analyzer, FLA-5000 (Fuji Photo Film), and MultiGauge software (Fuji Photo Film).

siRNA-treated HeLa cells were cultured in the presence of 1 μCi/ml of [^{32}P]P_i for 24 h. After incubation, cells were trypsinized and resuspended in 200 μl of PBS. The cell suspensions were sequentially mixed with 750 μl of chloroform/methanol (1:2, v/v), 250 μl of chloroform, and 250 μl of 0.1 M HCl/0.1 M KCl. The organic phase was obtained by centrifugation at 3000 × *g* for 2 min. Samples containing equivalent radioactivity were separated by TLC and then analyzed as described above.

Immunoblotting

Proteins were electrophoretically transferred from SDS-PAGE gels to nitrocellulose membranes (Bio-Rad) in blotting buffer (25 mM Tris, 192 mM glycine, 20% methanol) at a constant voltage of 15 V for 1 h. Membranes were blocked with blocking buffer (PBS containing 0.05% Tween 20 and 2% skim milk), incubated with primary antibodies in blocking buffer overnight at 4 °C, and washed three times with PBS containing 0.05% Tween 20. Membranes were then incubated with HRP-conjugated secondary antibodies for 1 h and washed three times with PBS containing 0.05% Tween 20. Signals were detected with a WSE-6100 LuminoGraph (ATTO). For the quantification of signals, ImageJ software (National Institutes of Health) was used.

Protein extraction from yeast cells

Yeast cells growing in the medium indicated were harvested, washed with H_2O, and then resuspended in 1 ml of H_2O. 150 μl of 2 M NaOH/8% 2-mercaptoethanol was added to the cell suspensions, and the mixtures were incubated on ice for 10 min. 75 μl of 100% TCA was added to the samples, which were then further incubated on ice for 10 min. After incubation, the proteins were precipitated by centrifugation at 20,000 × *g* for 2 min. The precipitates were resuspended in 1 ml acetone, followed by centrifugation at 20,000 × *g* for 2 min. The precipitates were then resuspended in SDS sample buffer and subjected to immunoblotting.

Chemical cross-linking of mitochondria

Isolated mitochondria were resuspended in SEM buffer (10 mM MOPS KOH, pH 7.2, 250 mM sucrose, 1 mM EDTA) to a concentration of 1 mg/ml and then treated with 1 mM DSP (Nacalai Tesque) at 26 °C for 15 min. After cross-linking, DSP was quenched with 100 mM Tris-HCl (pH 8.0). Cross-linked mitochondria were then re-isolated by centrifugation at 20,000 × *g* for 5 min and subjected to immunoprecipitation assaying as described below.

Immunoprecipitation and MS

For immunoprecipitation with anti-FLAG agarose under native conditions, yeast mitochondria were solubilized with lysis buffer (20 mM Hepes-KOH, pH 7.4, 100 mM KCl, 10% glycerol, 1% digitonin, and complete mini EDTA-free (Roche)). The lysates were incubated with anti-FLAG M2 agarose (Sigma-Aldrich) at 4 °C for 2 h. After washing the beads with lysis buffer three times, immunoprecipitates were eluted with 2% SDS or FLAG peptide. The eluates were analyzed by silver staining or immunoblotting. A protein band corresponding to ~28 kDa visualized on silver staining was subjected to in-gel digestion with trypsin and then analyzed by MS using OrbitrapVelos Pro (Thermo Fisher Scientific). The MS was conducted by Mizuho Oda and Emiko Koba (Laboratory for Technical Support, Medical Institute of Bioregulation, Kyushu University).

For immunoprecipitation with anti-FLAG M2 agarose under denaturing conditions, yeast mitochondria were solubilized with 50 μl of buffer comprising 50 mM Tris-HCl (pH 7.4) and 1% SDS at 70 °C for 10 min. The lysates were diluted with 500 μl of dilution buffer (50 mM Tris-HCl, pH 7.4, 150 mM NaCl, 10% glycerol, and 1% Triton X-100). After centrifugation at 20,000 × *g* for 10 min, the samples were incubated with anti-FLAG agarose for 2 h. After washing the beads with wash buffer (50 mM Tris-HCl, pH 7.4, 150 mM NaCl, 10% glycerol, 1% Triton X-100, and 0.1% SDS) three times, the immunoprecipitates were eluted with 2% SDS at 70 °C for 10 min. The eluates were analyzed by immunoblotting.

For immunoprecipitation with anti-Mdm35 antibodies, yeast mitochondria cross-linked with 1 mM DSP were solubilized with lysis buffer (20 mM Hepes-KOH, pH 7.4, 100 mM KCl, 10% glycerol, and 1% digitonin). The lysates were incubated with anti-Mdm35 antibodies for 1 h. After incubation, the antigen-antibody complexes were precipitated with Protein G Sepharose (Sigma-Aldrich). The immunoprecipitates were analyzed by immunoblotting.

Antibodies

We used mouse antibodies against yeast Por1 (Invitrogen), yeast Pgk1 (Invitrogen), FLAG M2 (Sigma-Aldrich), the MYC epitope (Invitrogen), and human actin (Santa Cruz Biotechnology); rabbit antibodies against yeast Tom70, yeast Mdm35 (11) (gift from Toshiya Endo and Yasushi Tamura); human Hsp60 (Santa Cruz Biotechnology) and human VDAC1 (Abcam); and goat antibodies against human VDAC2 (Abcam).

Measurement of glucose concentrations

Glucose concentrations in culture medium were measured by means of an F-kit D-glucose assay kit (Roche/R-Biopharm) according to the manufacturer's protocol.

Quantification and statistical analysis

The results of quantitative experiments are shown as means for independent experiments performed multiple times as indicated. The statistical significance of mean differences was assessed by means of the two-tailed Student's *t* test.

Author contributions—N. M. conceptualization; N. M. and S. F. data curation; N. M. formal analysis; N. M. and O. K. funding acquisition; N. M. investigation; N. M. methodology; N. M. writing-original draft; N. M. project administration; O. K. resources; O. K. supervision; O. K. writing-review and editing.

Acknowledgments—We thank Toshiya Endo and Yasushi Tamura for providing the anti-Tom70 and anti-Mdm35 antibodies, and for the helpful advice. We also thank Tadashi Ogishima, Motohiro Tani, Takeru Nose, Keitaro Suyama, and Hitoshi Kesamaru for the discussions. The MS was conducted by Mizuho Oda and Emiko Koba (Laboratory for Technical Support, Medical Institute of Bioregulation, Kyushu University).

References

1. Tamura, Y., Sesaki, H., and Endo, T. (2014) Phospholipid transport via mitochondria. *Traffic* **15,** 933–945 CrossRef Medline
2. Daum, G., Lees, N. D., Bard, M., and Dickson, R. (1998) Biochemistry, cell biology and molecular biology of lipids of *Saccharomyces cerevisiae*. *Yeast.* **14,** 1471–1510 CrossRef Medline
3. Jiang, F., Rizavi, H. S., and Greenberg, M. L. (1997) Cardiolipin is not essential for the growth of *Saccharomyces cerevisiae* on fermentable or non-fermentable carbon sources. *Mol. Microbiol.* **26,** 481–491 CrossRef Medline
4. Chang, S. C., Heacock, P. N., Mileykovskaya, E., Voelker, D. R., and Dowhan, W. (1998) Isolation and characterization of the gene (*CLS1*) encoding cardiolipin synthase in *Saccharomyces cerevisiae*. *J. Biol. Chem.* **273,** 14933–14941 CrossRef Medline
5. Trotter, P. J., Pedretti, J., and Voelker, D. R. (1993) Phosphatidylserine decarboxylase from *Saccharomyces cerevisiae*. Isolation of mutants, cloning of the gene, and creation of a null allele. *J. Biol. Chem.* **268,** 21416–21424 Medline
6. Clancey, C. J., Chang, S. C., and Dowhan, W. (1993) Cloning of a gene (*PSD1*) encoding phosphatidylserine decarboxylase from *Saccharomyces cerevisiae* by complementation of an *Escherichia coli* mutant. *J. Biol. Chem.* **268,** 24580–24590 Medline
7. Tuller, G., Hrastnik, C., Achleitner, G., Schiefthaler, U., Klein, F., and Daum, G. (1998) YDL142c encodes cardiolipin synthase (Cls1p) and is non-essential for aerobic growth of *Saccharomyces cerevisiae*. *FEBS Lett.* **421,** 15–18 CrossRef Medline
8. Tamura, Y., Harada, Y., Nishikawa, S. I., Yamano, K., Kamiya, M., Shiota, T., Kuroda, T., Kuge, O., Sesaki, H., Imai, K., Tomii, K., and Endo, T. (2013) Tam41 is a CDP-diacylglycerol synthase required for cardiolipin biosynthesis in mitochondria. *Cell Metab.* **17,** 709–718 CrossRef Medline
9. Kornmann, B., Currie, E., Collins, S. R., Schuldiner, M., Nunnari, J., Weissman, J. S., and Walter, P. (2009) An ER-mitochondria tethering complex revealed by a synthetic biology screen. *Science* **325,** 477–481 CrossRef Medline
10. Lahiri, S., Chao, J. T., Tavassoli, S., Wong, A. K., Choudhary, V., Young, B. P., Loewen, C. J., and Prinz, W. A. (2014) A conserved endoplasmic reticulum membrane protein complex (EMC) facilitates phospholipid transfer from the ER to mitochondria. *PLoS Biol.* **12,** e1001969 CrossRef Medline
11. Watanabe, Y., Tamura, Y., Kawano, S., and Endo, T. (2015) Structural and mechanistic insights into phospholipid transfer by Ups1-Mdm35 in mitochondria. *Nat. Commun.* **6,** 7922 CrossRef Medline
12. Connerth, M., Tatsuta, T., Haag, M., Klecker, T., Westermann, B., and Langer, T. (2012) Intramitochondrial transport of phosphatidic acid in yeast by a lipid transfer protein. *Science* **338,** 815–818 CrossRef Medline
13. Aaltonen, M. J., Friedman, J. R., Osman, C., Salin, B., di Rago, J. P., Nunnari, J., Langer, T., and Tatsuta, T. (2016) MIC OS and phospholipid transfer by Ups2-Mdm35 organize membrane lipid synthesis in mitochondria. *J. Cell Biol.* **213,** 525–534 CrossRef Medline
14. Miyata, N., Watanabe, Y., Tamura, Y., Endo, T., and Kuge, O. (2016) Phosphatidylserine transport by Ups2-Mdm35 in respiration-active mitochondria. *J. Cell Biol.* **214,** 77–88 CrossRef Medline
15. Tamura, Y., Iijima, M., and Sesaki, H. (2010) Mdm35p imports Ups proteins into the mitochondrial intermembrane space by functional complex formation. *EMBO J.* **29,** 2875–2887 CrossRef Medline
16. Potting, C., Wilmes, C., Engmann, T., Osman, C., and Langer, T. (2010) Regulation of mitochondrial phospholipids by Ups1/PRELI-like proteins depends on proteolysis and Mdm35. *EMBO J.* **29,** 2888–2898 CrossRef Medline
17. Tamura, Y., Endo, T., Iijima, M., and Sesaki, H. (2009) Ups1p and Ups2p antagonistically regulate cardiolipin metabolism in mitochondria. *J. Cell Biol.* **185,** 1029–1045 CrossRef Medline
18. Osman, C., Haag, M., Potting, C., Rodenfels, J., Dip, P. V., Wieland, F. T., Brügger, B., Westermann, B., and Langer, T. (2009) The genetic interactome of prohibitins: Coordinated control of cardiolipin and phosphatidylethanolamine by conserved regulators in mitochondria. *J. Cell Biol.* **184,** 583–596 CrossRef Medline
19. Harner, M., Körner, C., Walther, D., Mokranjac, D., Kaesmacher, J., Welsch, U., Griffith, J., Mann, M., Reggiori, F., and Neupert, W. (2011) The mitochondrial contact site complex, a determinant of mitochondrial architecture. *EMBO J.* **30,** 4356–4370 CrossRef Medline
20. Tamura, Y., Onguka, O., Hobbs, A. E., Jensen, R. E., Iijima, M., Claypool, S. M., and Sesaki, H. (2012) Role for two conserved intermembrane space proteins, Ups1p and Ups2p, in intra-mitochondrial phospholipid trafficking. *J. Biol. Chem.* **287,** 15205–15218 CrossRef Medline
21. Mihara, K., and Sato, R. (1985) Molecular cloning and sequencing of cDNA for yeast porin, an outer mitochondrial membrane protein: A search for targeting signal in the primary structure. *EMBO J.* **4,** 769–774 CrossRef Medline
22. Lee, A. C., Xu, X., Blachly-Dyson, E., Forte, M., and Colombini, M. (1998) The role of yeast VDAC genes on the permeability of the mitochondrial outer membrane. *J. Membr. Biol.* **161,** 173–181 CrossRef Medline
23. Blachly-Dyson, E., Song, J., Wolfgang, W. J., Colombini, M., and Forte, M. (1997) Multicopy suppressors of phenotypes resulting from the absence of yeast VDAC encode a VDAC-like protein. *Mol. Cell. Biol.* **17,** 5727–5738 CrossRef Medline
24. Dimmer, K. S., Jakobs, S., Vogel, F., Altmann, K., and Westermann, B. (2005) Mdm31 and Mdm32 are inner membrane proteins required for maintenance of mitochondrial shape and stability of mitochondrial DNA nucleoids in yeast. *J. Cell Biol.* **168,** 103–115 CrossRef Medline
25. Bellí, G., Garí, E., Aldea, M., and Herrero, E. (1998) Functional analysis of yeast essential genes using a promoter-substitution cassette and the tetracycline-regulatable dual expression system. *Yeast* **14,** 1127–1138 CrossRef3.0.CO%3B2-# Medline
26. Miyata, N., Goda, N., Matsuo, K., Hoketsu, T., and Kuge, O. (2017) Cooperative function of Fmp30, Mdm31, and Mdm32 in Ups1-independent cardiolipin accumulation in the yeast *Saccharomyces cerevisiae*. *Sci. Rep.* **7,** 16447 CrossRef Medline
27. Tomasello, M. F., Guarino, F., Reina, S., Messina, A., and De Pinto, V. (2013) The Voltage-dependent anion selective channel 1 (VDAC1) topography in the mitochondrial outer membrane as detected in intact cell. *PLoS One* **8,** e81522 CrossRef Medline
28. Checchetto, V., Reina, S., Magrì, A., Szabo, I., and De Pinto, V. (2014) Recombinant human voltage dependent anion selective channel isoform 3 (hVDAC3) forms pores with a very small conductance. *Cell. Physiol. Biochem.* **34,** 842–853 CrossRef Medline

29. Messina, A., Reina, S., Guarino, F., and De Pinto, V. (2012) VDAC isoforms in mammals. *Biochim. Biophys. Acta* **1818,** 1466–1476 CrossRef Medline
30. Gawaz, M., Douglas, M. G., and Klingenberg, M. (1990) Structure-function studies of adenine nucleotide transport in mitochondria. II. Biochemical analysis of distinct AAC1 and AAC2 proteins in yeast. *J. Biol. Chem.* **265,** 14202–14208 Medline
31. Van Dyck, E., Jank, B., Ragnini, A., Schweyen, R. J., Duyckaerts, C., Sluse, F., and Foury, F. (1995) Overexpression of a novel member of the mitochondrial carrier family rescues defects in both DNA and RNA metabolism in yeast mitochondria. *Mol. Gen. Genet.* **246,** 426–436 CrossRef Medline
32. Kmita, H., and Budzińska, M. (2000) Involvement of the TOM complex in external NADH transport into yeast mitochondria depleted of mitochondrial porin1. *Biochim. Biophys. Acta* **1509,** 86–94 CrossRef Medline
33. Kuroda, T., Tani, M., Moriguchi, A., Tokunaga, S., Higuchi, T., Kitada, S., and Kuge, O. (2011) FMP30 is required for the maintenance of a normal cardiolipin level and mitochondrial morphology in the absence of mitochondrial phosphatidylethanolamine synthesis. *Mol. Microbiol.* **80,** 248–265 CrossRef Medline
34. Sesaki, H., Dunn, C. D., Iijima, M., Shepard, K. A., Yaffe, M. P., Machamer, C. E., and Jensen, R. E. (2006) Ups1p, a conserved intermembrane space protein, regulates mitochondrial shape and alternative topogenesis of Mgm1p. *J. Cell Biol.* **173,** 651–658 CrossRef Medline
35. Lorenz, M. C., Muir, R. S., Lim, E., McElver, J., Weber, S. C., and Heitman, J. (1995) Gene disruption with PCR products in *Saccharomyces cerevisiae*. *Gene* **158,** 113–117 CrossRef Medline
36. Blachly-Dyson, E., Zambronicz, E. B., Yu, W. H., Adams, V., McCabe, E. R., Adelman, J., Colombini, M., and Forte, M. (1993) Cloning and functional expression in yeast of two human isoforms of the outer mitochondrial membrane channel, the voltage-dependent anion channel. *J. Biol. Chem.* **268,** 1835–1841 Medline
37. Janke, C., Magiera, M. M., Rathfelder, N., Taxis, C., Reber, S., Maekawa, H., Moreno-Borchart, A., Doenges, G., Schwob, E., Schiebel, E., and Knop, M. (2004) A versatile toolbox for PCR-based tagging of yeast genes: New fluorescent proteins, more markers and promoter substitution cassettes. *Yeast.* **21,** 947–962 CrossRef Medline
38. Vaden, D. L., Gohil, V. M., Gu, Z., and Greenberg, M. L. (2005) Separation of yeast phospholipids using one-dimensional thin-layer chromatography. *Anal. Biochem.* **338,** 162–164 CrossRef Medline